Research Article

Esraa Hamdy, Hamada El-Gendi, Abdulaziz Al-Askar, Ali El-Far, Przemysław Kowalczewski, Said Behiry, Ahmed Abdelkhalek*

Copper oxide nanoparticles-mediated *Heliotropium bacciferum* leaf extract: Antifungal activity and molecular docking assays against strawberry pathogens

https://doi.org/10.1515/chem-2024-0028
received March 16, 2024; accepted April 10, 2024

Abstract: In the current study, *Heliotropium bacciferum* leaf extract was used to biosynthesize copper oxide nanoparticles (CuO-NPs). Various analytical techniques were used to characterize the produced CuO-NPs. Transmission electron microscope investigation indicated well-distributed spherical particles in various development phases. The particles' diameters ranged from 22.15 to 37.01 nm, with an average of 24.8 ± 6.1 nm. Energy dispersive X-ray examination confirmed the presence of nanoscale Cu ions at a high concentration, as seen by the strong signal peak at 1 keV. Fourier transform infrared spectrum revealed various functional groups on the green-produced CuO-NPs, as evidenced by multiple absorption beaks. The bands found at 3,195 and 2,916 cm^{-1} revealed that phenolic and flavonoid compounds' alcohols and alkanes were stretching C–H. Also, a band at 1,034 cm^{-1} is typically attributed to CuO production. CuO-NPs exhibited significant bioactivity against isolated and molecularly identified fungal strains, including *Rhizoctonia solani* (OR116528), *Fusarium oxysporum* (OR116508), and *Botrytis cinerea* (OR116491). Remarkably, the highest inhibition percentages were recorded at 100 µg/mL, with values 81.48, 71.11, and 50.74% for *R. solani*, *F. oxysporum*, and *B. cinerea*, respectively. Molecular docking interactions revealed that the highest binding affinity of CuO-NPs was −5.1 for the oxidoreductase of *B. cinerea* and −5.2 and −5.4 for the chitin synthase of *R. solani* and *F. oxysporum*, respectively. Consequentially, the biosynthesized CuO-NPs could be employed as antifungal biocontrol agents, as well as using *H. bacciferum* leaf extract for the synthesis of nanoparticles for various sustainable agricultural applications.

Keywords: copper oxide nanoparticles, *Heliotropium bacciferum*, green synthesis, antifungal activity, plant disease, molecular docking

*** Corresponding author: Ahmed Abdelkhalek,** Plant Protection and Biomolecular Diagnosis Department, Arid Lands Cultivation Research Institute, City of Scientific Research and Technological Applications, New Borg El-Arab City, 21934, Egypt, e-mail: abdelkhalek2@yahoo.com, tel: +20 1007556883
Esraa Hamdy: Plant Protection and Biomolecular Diagnosis Department, Arid Lands Cultivation Research Institute, City of Scientific Research and Technological Applications, New Borg El-Arab City, 21934, Egypt, e-mail: esraah752@gmail.com
Hamada El-Gendi: Bioprocess Development Department, Genetic Engineering and Biotechnology Research Institute, City of Scientific Research and Technological Applications, New Borg El-Arab City, 21934, Egypt, e-mail: elgendi1981@gmail.com
Abdulaziz Al-Askar: Department of Botany and Microbiology, College of Science, King Saud University, P.O. Box 2455, Riyadh, 11451, Saudi Arabia, e-mail: aalaskara@ksu.edu.sa
Ali El-Far: Department of Biochemistry, Faculty of Veterinary Medicine, Damanhour University, Damanhour, 22511, Egypt, e-mail: ali.elfar@damanhour.edu.eg
Przemysław Kowalczewski: Department of Food Technology of Plant Origin, Poznań University of Life Sciences, Poznań, Poland, e-mail: przemyslaw.kowalczewski@up.poznan.pl
Said Behiry: Agricultural Botany Department, Faculty of Agriculture (Saba Basha), Alexandria University, Alexandria, 21531, Egypt, e-mail: said.behiry@alexu.edu.eg

1 Introduction

Nanotechnology is an important field of study in medicine, food, health, the chemical industry, electronics, energy science, cosmetics, space exploration, and environmental sciences [1,2]. The demand for nanotechnology-derived products is increasing, and this emerging technology has the potential to benefit human health [3]. Nanoparticle (NP) biosynthesis has recently emerged as a more cost-effective and environmentally friendly alternative to chemical and physical methods [4,5]. Plant-based extracts are the most promising biological alternative [6,7], where they

are inexpensive "chemical factories" that require minimal maintenance. However, applying phyto-NPs in medical, pharmaceutical, cosmetic, and agricultural fields still has a long way to go. Green chemistry-based NP synthesis is a single-step process requiring less energy to fabricate eco-friendly NPs that can convert agricultural waste and food into energy and other useful products [8]. The process of converting metal ions into NPs is greatly aided by plant-derived compounds, including terpenoids, tannins, alkaloids, steroids, saponins, and polyphenols [9]. The investigation of functional groups found in aqueous plant leaf extracts has previously been conducted to assess their potential utility as reducing agents. As a result, various functional groups, including amines, polyphenols, and carboxylic acids, present in plant leaf extracts have been employed as reducing agents in synthesizing silver NPs [10].

Copper oxide NPs possess unique crystal structures and high surface areas, making them highly valuable antimicrobial agents. These NPs are robust and stable and have a longer shelf life than other organic antimicrobial agents [11]. Various methods of CuO synthesis exist, such as chemical precipitation, microwave irradiation, and thermal decomposition. The chemical method, on the other hand, uses dangerous chemicals that limit its uses. This has led to more interest in biological methods for synthesizing CuO-NPs, which are better for the environment and easier to handle and do not require cell culture [12]. Thus, researchers have already reported using plant extracts such as *Punica granatum* [13], *Ficus sycomorus* [7], *Malva sylvestris* [14], and *Ocimum basilicum* [15] for the synthesis of oxide NPs. The biosynthesized CuO-NPs were subjected to characterization using a range of physicochemical techniques, such as Fourier-transform infrared spectroscopy (FTIR), X-ray diffraction, and electron microscopes. Furthermore, the synthesized CuO-NPs were employed in diverse applications, including antibacterial and antifungal activities [16–20].

Green NP production with *Heliotropium bacciferum* leaf extract is an intriguing strategy that takes advantage of the natural features of plant extracts to produce NPs. *H. bacciferum* (Boraginaceae family), sometimes known as the "*Cherry Heliotrope*," is a medicinal plant that contains several bioactive chemicals, including polyphenols, flavonoids, alkaloids, and terpenoids [21]. These chemicals can be used as reducing agents and stabilizers in the manufacture of NPs. The Boraginaceae family has a wide range of flavonoids and polyphenols, which have been shown to have a variety of pharmacological actions, including antibacterial, antioxidant, anti-inflammatory, antiviral, and hepatoprotective characteristics [22]. *H. bacciferum* has been recognized as a rich reservoir of various phytochemicals, with notable efficiency in scavenging diphenyl picryl hydrazyl radicals, as described in previous investigations [23]. A recent investigation showed that the aerial components of *H. bacciferum* have significant antibacterial and antifungal activities [24]. The antifungal capabilities of specific components of the *H. bacciferum* plant are not well researched. As a result, the primary goal of this research was to determine the efficacy of copper NPs generated from *H. bacciferum* leaf extract in preventing fungal development. Furthermore, the characterization of biogenic NPs for research purposes necessitates the use of a variety of instruments and analytical procedures. In addition, the CuO-NPs were molecularly docked with fungal chitin synthase, cutinase agglutinin, trypsin, and oxidoreductase.

2 Materials and methods

2.1 Green synthesis of CuO-NPs through *H. bacciferum* leaves extract

The green synthesis of CuO-NPs was mediated through *H. bacciferum* leaf extract using cupric sulfate ($CuSO_4$, Sigma-Aldrich, USA) as a precursor according to the method described by Chen et al. [25] with simple modifications. Briefly, the plant extract was homogenized (150 rpm) for 3 h at 50°C in 100 mM phosphate buffer with a final solid-to-liquid ratio of 10%. Afterward, the clear supernatant was separated through centrifugation for 15 min at 10,000 rpm and used as a source for reduction power. The $CuSO_4$ reduction was carried out by mixing $CuSO_4$ solution (10 mM) with clear plant extract in a ratio of 1:1 for 5 h under shaking at 50°C. After cooling at room temperature, the CuO-NPs formation was indicated by a dark brownish-to-black color developing in the reduction mixer. The developed CuO-NPs were separated through centrifugation at 10,000 rpm for 15 min. To assure purity, the precipitated CuO-NPs were washed several times with double distilled water (ddH_2O) and finally with 95% ethanol before being dried at 80°C for 24 h before any further processing.

2.2 Characterization of prepared CuO-NPs

The surface morphology and size of the eco-friendly synthesized CuO-NPs were studied through transmission electron microscopy (TEM) using the JSM-6360 microscope (JEOL, Tokyo, Japan), operating at 15 kV as an acceleration voltage with a carbon-coated copper grid used for sample loading. The energy dispersive X-ray (EDX) unit of TEM (JSM-6360 microscope; JEOL, Tokyo, Japan) was used to evaluate the

elemental analysis of the prepared CuO-NPs. The net surface charge (zeta potential) of the prepared NPs was evaluated through Zetasizer nanoseries (ZS, Malvern, Germany). The hydrodynamic size of the prepared CuO-NPs in colloidal solution was evaluated at two angles, 11 and 90°, through Malvern Zetasizer (ZS). Furthermore, the surface functional groups of CuO-NPs were examined utilizing the KBr-disc technique for FTIR spectroscopy at 400–4,000 cm^{-1}.

2.3 Plant pathogens' isolation and preliminary identification

The isolation and identification of pathogenic fungi from strawberry plants were performed in different steps. First, plants exhibiting symptoms such as wilting, yellowing, discoloration, lesions, or abnormal growth were collected, and the roots or fruits were separated and cut into pieces. Then, a 1% (v/v) aqueous solution of sodium hypochlorite was used to sterilize the symptomatic pieces. Afterward, the small pieces were placed on potato dextrose agar (PDA) plates and incubated at 25–28°C for a week. Any plate exhibiting fungal growth was then purified and subjected to macroscopic examination, including color, texture, shape, and growth patterns, to identify the fungal species.

2.4 Molecular identification

For molecular identification, the ITS region was amplified from the isolated fungi. The extraction process began with 4-day fungal cultures, from which fungal DNA was extracted using the CTAB-DNA extraction method [26,27]. Following DNA extraction, a polymerase chain reaction (PCR) was performed to amplify the ITS region of the fungal ribosomal DNA using ITS1 and ITS4 primers [28]. Gel electrophoresis was carried out to separate the PCR products. After gel electrophoresis, the fungal-PCR amplicons were purified using a commercial purification kit (ChargeSwitch™ gDNA Plant Kit, Thermo Fisher Scientific, Carlsbad, CA, USA). The purified fragments were subsequently sent to a sequencing service provider (Macrogen Co., Seoul, Korea) for DNA sequencing utilizing Sanger sequencing technology. Upon obtaining the ITS-DNA sequence data, it underwent analysis and comparison with the reference database GenBank using sequence alignment algorithms. The BLAST tool (https://blast.ncbi.nlm.nih.gov/Blast.cgi) assisted in fungal species identification based on sequence similarity. The identified pathogenic fungi from strawberry plants were further studied to understand potential control measures.

2.5 Antimicrobial activities of the synthesized NPs

The food poison technique [29] was used to evaluate the antifungal activity of potential antifungal agents against the isolated fungi from strawberry plants. The biosynthesized CuO-NPs were prepared at 25, 50, 75, and 100 µg/mL in final concentrations. They were incorporated into a suitable solid culture medium, PDA, by being thoroughly mixed while the medium was still in a liquid state, after which the medium was poured into Petri dishes and allowed to solidify. A small plug of the isolated fungal strains was transferred onto the center of the agar plates containing the CuO-NPs using a sterile toothpick. For comparison purposes, control plates containing the culture PDA medium without the CuO-NPs were inoculated. The plates were incubated under appropriate conditions for fungal growth (25–28°C) for 7 days until sufficient fungal growth was observed in the control plates. The plates were examined, and the growth of the test fungi on the plates containing the synthesized CuO-NPs was compared with that on the control plates. The degree of inhibition was evaluated by measuring the diameter of the fungal colonies and comparing them to the control colonies. The inhibition percentage (IP) was calculated as IP% = [(control-fungal treatment)/control] × 100.

2.6 Molecular docking

Before docking, the target proteins were retrieved from the RCSB Protein Data Bank (https://www.rcsb.org/) and AlphaFold Protein Structure (https://alphafold.ebi.ac.uk/) databases. Furthermore, the target proteins were prepared by removing water molecules and attaching ligands by the UCSF Chimera software package. At the same time, the CuO structure was retrieved in the crystallographic information framework from the Material Project database (https://next-gen.materialsproject.org/) and converted to PDB format using Open Babel software. The molecular docking interaction of CuO and target proteins in *Rhizoctonia solani* (chitin synthase, cutinase, and agglutinin), *Fusarium oxysporum* (chitin synthase, cutinase, and trypsin), and *Botrytis cinerea* (chitin synthase, cutinase, and oxidoreductase) were done using AutoDock 4.2 tool and UCSF Chimera, while visualized by BIOVIA Discovery Studio software.

3 Results and discussion

3.1 Particle morphology, size, and elemental analysis through TEM

The surface morphology and size of the prepared CuO-NPs were evaluated through TEM. Figure 1a shows that the prepared CuO-NPs revealed well-dispersed spherical particles in different growth phases. The prepared particles revealed varied sizes ranging from 22.15 to 37.01 nm with an average size of 24.8 ± 6.1 nm (Figure 1b), which asserted the ability of *H. bacciferum* leaf extract to reduce Cu ions to nanoscale. The CuO-NPs of the same size were reported in other studies [30,31]. The TEM results also indicated a significant separation of all particles from each other with limited aggregation. Furthermore, all particles were surrounded with secondary material in a cap-like shape, which could be attributed to the organic material from plant extract as reported in several studies [32–34]. Additionally, the EDX analysis was applied to evaluate the elemental nature of the prepared CuO-NPs. The analysis (Figure 1c) revealed the existence of copper (Cu) and oxygen (O) constituents in copper oxide NPs. The occurrence of strong and narrow diffraction peaks in the EDS spectrum indicates the crystalline quality of the product [35]. The peak observed at 0.5 keV indicates the presence of oxygen, whereas the peaks observed at binding energy values of 1.0, 8.0, and 9.0 keV provide confirmation of the presence of copper [19,35,36]. In addition, the presence of a carbon atom was seen at an energy level of around 0.2 keV, which can be attributed to the organic layer present in the synthesized CuO-NPs [36]. The presence of sulfur may be attributed to the utilization of copper sulfate as the initial substance [37].

3.2 Zeta potential and particle distribution

The surface charge of NPs is an important characteristic that directly mediates the particle's stability, biosafety, and bioactivity [38]. Hence, the net surface charge of the prepared CuO-NPs was evaluated through Zetasizer. The results indicated in Figure 2a revealed positively charged CuO-NPs with an average zeta potential of about 24.8 ± 3.23 mV, which points to the stability of the prepared particles in the biological systems as the measured zeta potential within +30 and −30 mV [39,40]. The positively charged CuO-NPs were previously reported in several CuO-NPs prepared by various plant extracts, including *Stachys lavandulifolia* [41] and *Mussaenda frondosa* L. [39]. On the other hand, the Zetasizer was used to analyze the particle size distribution of the greenly synthesized CuO-NPs. As indicated in Figure 2b, the CuO-NPs ranged between 38.4 and 192.9 nm as measured at 11° and 90°, respectively. The particle size range is significantly higher than that detected through TEM analysis, which could be accredited to the non-homogeneous particle size (polydisperse nature) of the prepared particles and the fact that DSL measures particle size in the wet state. In contrast, the TEM measures the particle size in a dried condition [42,43].

3.3 FTIR analysis for prepared CuO-NPs

The functional groups on the CuO-NPs were evaluated through FTIR analysis, as shown in Figure 3 and Table 1. The FTIR spectrum revealed several functional groups on the green synthesized CuO-NPs indicated by several absorption beaks in the scanning range (4,000–400 cm^{-1}). The

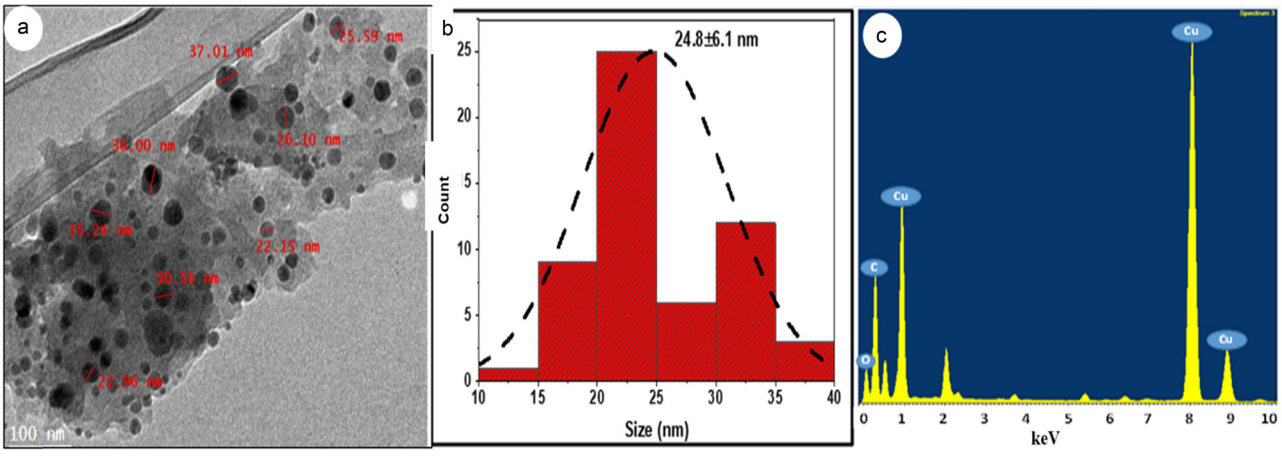

Figure 1: Surface morphology of the green synthesized CuO-NPs (a) as illustrated through transmission electron microscopy (TEM) with corresponding average particle size (b) calculated through ImageJ software. The prepared NPs' elemental analysis is illustrated through EDX unit (c).

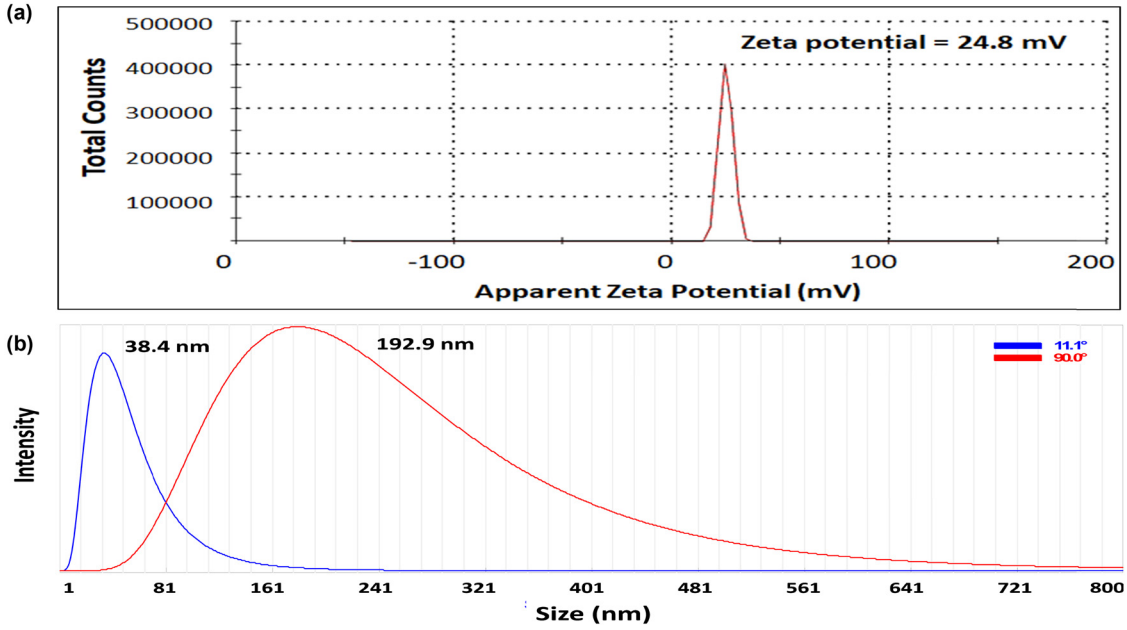

Figure 2: The surface net charge (zeta potential) of the prepared CuO-NPs (a) and hydrodynamic size at two different angles (b) as illustrated through Zetasizer.

bands detected at 3,195 and 2,916 cm^{-1} showed the C–H stretching of alcohols and alkanes of phenolic and flavonoid compounds [32,44]. Two small bands were also observed at 2,338 and 1,699 cm^{-1}, indicating O═C═O stretching and amide I bond of proteins/enzymes [45]. The three bands detected at 1,582, 1,426, and 1,325 cm^{-1} indicated the C═O stretching of alkanes, OH phenolic bending, and C–N stretching, respectively [32,44,46]. The band detected at 1,178 cm^{-1} indicated the observance of C–OH stretching and C–C stretching of alkanes [32]. The FTIR spectrum indicated a band around 1,034 cm^{-1}, which is usually attributed to CuO formation [36,47], whereas the band at 784 cm^{-1} is usually attributed to M–O vibration in the CuO structure [48]. Overall, the FTIR results demonstrated the presence of various phenolic substances, terpenoids, or proteins attached to the CuO NPs' surface, which are in line with the TEM results. The free

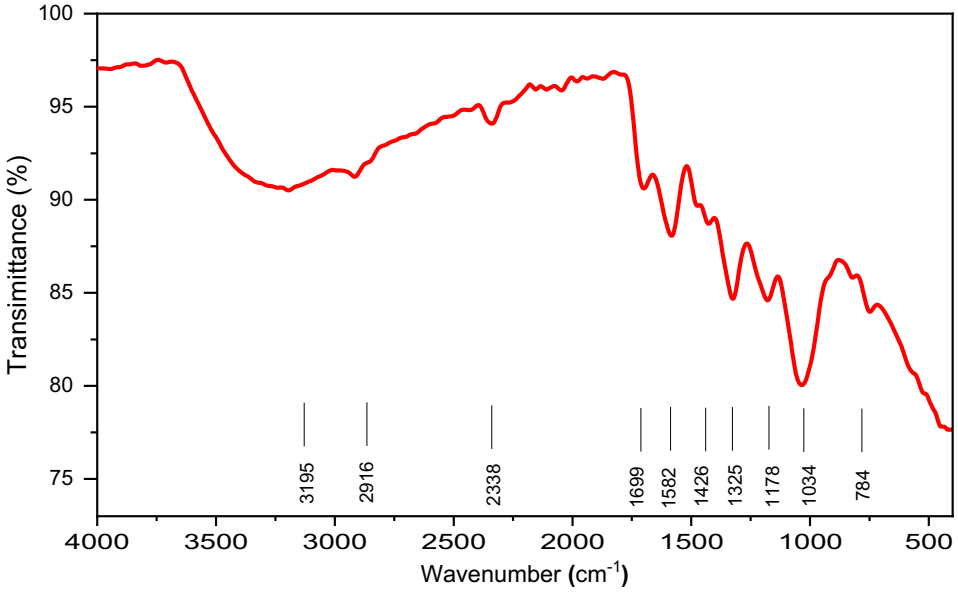

Figure 3: The FTIR spectra of green-synthesized CuO-NPs show various bands corresponding to distinct functional groups on the NP surface.

Table 1: FTIR spectra list of band positions for CuO-NPs in this study

Wave number (cm^{-1})	Band	Functional group	References
3,195	C–H stretch	Polyphenolic compounds	[50]
2,916	C–H stretch	Alkanes	[34,51]
2,338	O═C═O stretch	Carbon dioxide	[34]
1,699	–C═C– stretch	Alkenes	[51,52]
1,582	N–H bend	Amide I bonds (NH) of proteins	[32,53,54]
1,426	C–O stretch	Ester and aliphatic ether	[54,55]
1,325	O–H stretch	Phenolic group	[54]
1,178	C–OH bending	Alkanes	[32,51,52]
1,034	C–N stretch	Aliphatic and aromatic amines	[32,34]
784	Cu–O vibrations	Corroborating the formation of CuO-NPs	[48,56,57]

amino and carboxylic groups that have interacted with the copper surface (as an organic coat) may cause the stability of the green synthesized CuO-NPs to prevent their agglomeration [32,49].

3.4 Isolation and identification of the pathogenic fungi

The fungal isolates that had been obtained from infected strawberry plants were identified using morphological and molecular identification methods.

3.4.1 Symptoms and morphological identification

The morphological features of fungal colonies isolated from the plants were indicative of root rot symptoms, typically including a white to light brown color, irregular growth patterns, and a cottony to fluffy texture. Under the microscope, the fungus was characterized by its multinucleate hyphae without septa (aseptate) and the presence of sclerotia, which were compact masses of hyphae that appeared dark brown to black. All these features corresponded to the fungus *R. solani* [58,59].

The isolation trials conducted on symptomatic plants exhibiting wilt and yellowing of leaves revealed fungal colonies characterized by a cottony texture and white color. Microscopic analysis unveiled the presence of macroconidia, which displayed a sickle-shaped morphology with multicellular characteristics, exhibiting a curved and tapered appearance. Additionally, microconidia (small, oval, unicellular spores) and chlamydospores (thick-walled, round, survival structures) were evident. These morphological attributes were consistent with those associated with the fungus *F. oxysporum* as reported in previous studies [60,61]

The afflicted plants exhibited symptoms of fruit rot, commonly referred to as gray mold, with fungal colonies presenting a characteristic gray-to-brown coloration and a velvety to a fluffy texture. Microscopic examination revealed septate hyphae and the presence of conidiophores, which were branched structures responsible for bearing conidia (asexual spores). The conidia, typically oval-shaped, were produced in chains, delineating the characteristic features of *B. cinerea* [62,63].

3.4.2 Molecular identification

For molecular identification purposes, the ITS region of the ribosomal RNA gene cluster served as a common target. This region's widespread adoption stemmed from its high sequence variability across fungal species, rendering it instrumental for fungal identification and phylogenetic analyses. The PCR was employed to amplify the ITS region of fungal DNA, followed by DNA sequencing and subsequent comparison with known sequences within the GenBank public database. Sequencing of the PCR-amplified ITS region was conducted for each isolate, and the resulting sequences were juxtaposed with reference sequences in the database, affirming the identities of *R. solani*, *F. oxysporum*, and *B. cinerea* in the infected strawberry samples. These sequences were deposited in the GenBank database under accession numbers OR116528, OR116508, and OR116491, respectively. PCR is widely recognized for its exceptional accuracy in detecting and identifying diverse organisms, encompassing pathogenic and non-pathogenic fungi, such as *Alternaria alternata*, *F. solani*, *R. solani*, and *Aspergillus* spp. [64,65]. The nuclear ribosomal internal transcribed spacer (ITS) region has been accepted as the authoritative fungal barcode and represents mycology's most frequently examined genetic marker. The average length of the ITS region within the fungi kingdom is around 550 base pairs (bp). However, it

Table 2: Percentage of *in vitro* growth suppression of plant pathogenic fungi subjected to CuO-NPs biosynthesized from *H. bacciferum* leaf extract

Concentrations (µg/mL)	IP (%)		
	R. solani*	***F. oxysporum***	***B. cinerea***
25	78.15c	70.00a	40.37c
50	80.00b	70.37a	44.44bc
75	80.37b	70.74a	48.52ab
100	81.48a	71.11a	50.74a
Negative control	00.00d	00.00b	00.00d

*The different letters beside the antifungal means in each column indicate that the data were significantly other at probability level 0.05.

is essential to note that this length may differ substantially among various species [66]. The geographical area under consideration encompasses two distinct regions, referred to as ITS1 and ITS2, characterized by their variability. These regions are separated by the presence of the 5.8S ribosomal gene, which is conserved to a high degree. Including a chimera, control is essential in ITS-based mycological investigations due to the crucial role played by the 5.8S gene in facilitating chimeric elongation in mixed-template PCR [67]. In conclusion, the combination of morphological and molecular identification techniques confirmed the presence of the detected fungal strains in the infected strawberry samples. This information was crucial for understanding the diseases caused by these pathogens and developing effective control strategies for strawberry production.

3.5 Antimicrobial activities against the isolated fungi

Table 2 and Figure 4 show the inhibitory percentages of the three fungi (*R. solani*, *F. oxysporum*, and *B. cinerea*) at four different concentrations (25, 50, 75, and 100 µg/mL) of CuO-NPs biosynthesized from *H. bacciferum* leaf extract. A negative control group is included, indicating no inhibition of fungal growth. At the lowest 25 µg/mL concentration, *R. solani* showed 78.15% inhibition, *F. oxysporum* exhibited 70.00% inhibition, and *B. cinerea* displayed 40.37% inhibition. As the concentration of CuO-NPs increased to 50 µg/mL, the IPs for *R. solani*, *F. oxysporum*, and *B. cinerea* were 80.00, 70.37, and 44.44%, respectively. At 75 µg/mL concentration, *R. solani* had 80.37% inhibition, *F. oxysporum* showed 70.74% inhibition, and *B. cinerea* demonstrated 48.52% inhibition. Finally, at the highest 100 µg/mL concentration, the IPs were 81.48% for *R. solani*, 71.11% for *F. oxysporum*, and 50.74% for *B. cinerea*. The data suggest that the biosynthesized CuO-NPs from *H. bacciferum* leaf extract can potentially suppress the growth of plant pathogenic fungi. The IPs generally increased with higher concentrations of CuO-NPs, indicating a dose-dependent effect.

Nanomaterial synthesis typically employs three distinct approaches: physical, chemical, and biological processes. Plant-based nanotechnology has the potential to be cost-effective, biocompatible, dependable, and environmentally friendly. Green methods have recently gained prominence as a significant aspect of nanotechnology. Green-mediated production of nanomaterials is emerging

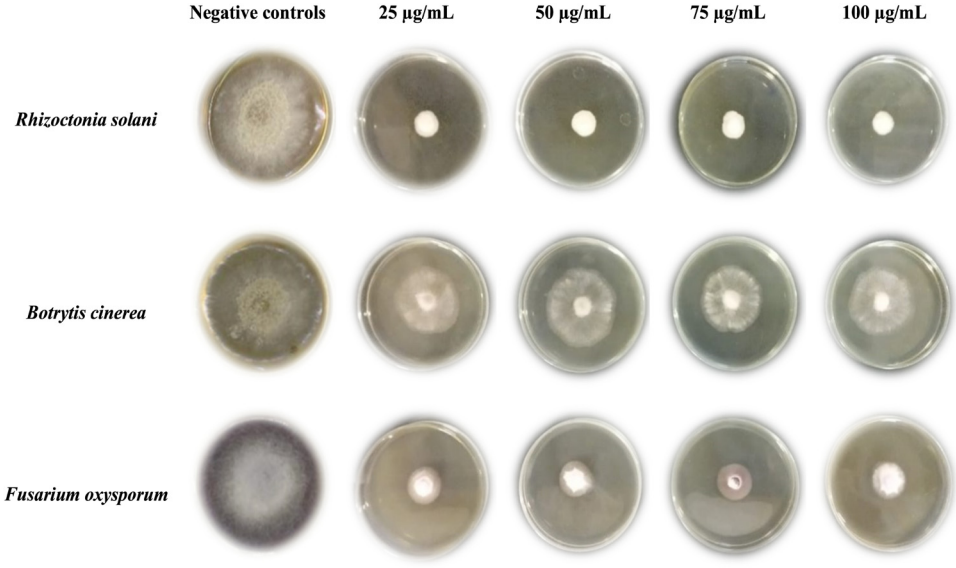

Figure 4: The antifungal activity of the CuO-NPs biosynthesized from *H. bacciferum* leaf extract against three fungi (*R. solani*, *F. oxysporum*, and *B. cinerea*).

Table 3: Molecular docking interaction of CuO and target proteins in *R. solani*, *F. oxysporum*, and *B. cinerea*

Fungi	Targets	Binding energy (kcal/mol)	Interactions
R. solani	Chitin synthase	−5.2	Hydrogen bonds: SER778, ARG781, TYR894, GLY905, and GLU906
	Cutinase	−4.3	Hydrogen bonds: THR11, LYS13, SER39, GLY41, and GLN45
	Agglutinin	−4.7	Hydrogen bonds: ARG88, ALA128, GLU131, and ASN155
F. oxysporum	Chitin synthase	−5.4	Hydrogen bonds: ASP385, PHE386, TYR389, SER395, and GLN497
	Cutinase	−5.1	Hydrogen bonds: SER43, ASN85, SER121, and GLN122
	Trypsin	−5.0	Hydrogen bonds: SER190, CYS191, SER214, TRP215, and VAL227
B. cinerea	Chitin synthase	−4.4	Hydrogen bonds: ASP385, PHE386, TYR389, SER395, and GLN497
	Cutinase	−4.8	Hydrogen bonds: ALA30, CYS31, SER32, SER67, and THR70
	Oxidoreductase	−5.1	Hydrogen bonds: THR35, PRO36, GLN38, GLN143, and GLN427

as an alternative approach. Various green sources have been documented, such as microorganisms, fungi, viruses, and plant extracts. Jebril et al. [68] utilized *Melia azedarach* leaf extract as a reducing agent to green synthesize silver nanoparticles (Ag-NPs). The synthesized Ag-NPs demonstrated antifungal activity by inhibiting the growth of *Verticillium dahlia* [68]. Mali et al. [17] employed *Celastrus paniculatus* leaf extract to produce cost-effective and eco-friendly copper nanoparticles (Cu-NPs) for copper reduction. The Cu-NPs displayed significant antifungal properties against *F. oxysporum* [17]. Zhu et al. [69] used *Cinnamomum camphora* leaf extract for the green synthesis of zinc nanoparticles (Zn-NPs). The synthesized Zn-NPs exhibited antifungal activity against *Alternaria alternate*, inhibiting spore germination and causing cell membrane disruption. This disruption resulted in the leakage of essential proteins and nucleic acids, leading to the death of the fungal pathogen [69].

Numerous research teams have used plant leaf extracts to biosynthesize Ag-NPs and explored their antibacterial applications [70–72]. Ravichandran et al. discovered that *Parkia speciosa* leaf extract could be utilized for the green chemistry-based synthesis of Ag-NPs with antimicrobial properties, which may be employed to treat various diseases [73]. Punniyakotti et al. [74] produced Cu-NPs using *Cardiospermum halicacabum* leaf extracts and found that Cu-NPs possess antibacterial properties, disrupting the bacterial cell wall and hindering their growth within the host body [74]. Mukherjee et al. [75] showed that *Olax scandens* leaf extract could be used to make Ag-NPs using green chemistry. They revealed that the Ag-NPs can be applied in four distinct

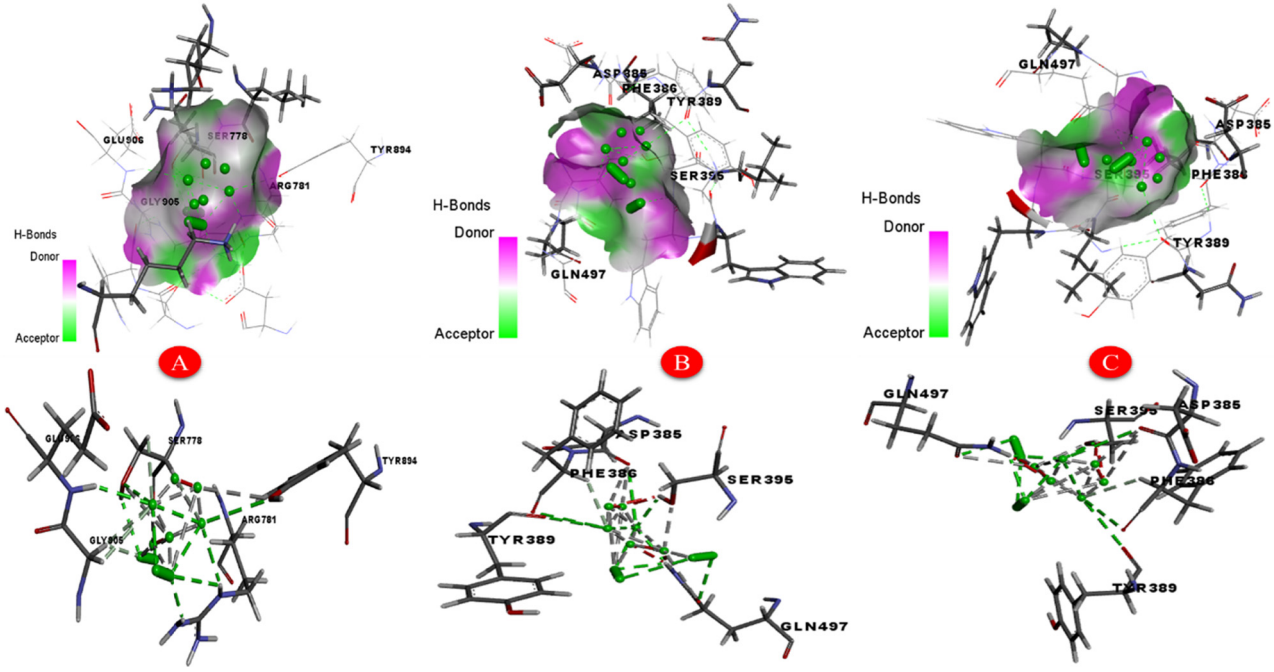

Figure 5: Molecular interaction of CuO-NPs and chitin synthase of *R. solani* (a), *F. oxysporum* (b), and *B. cinerea* (c).

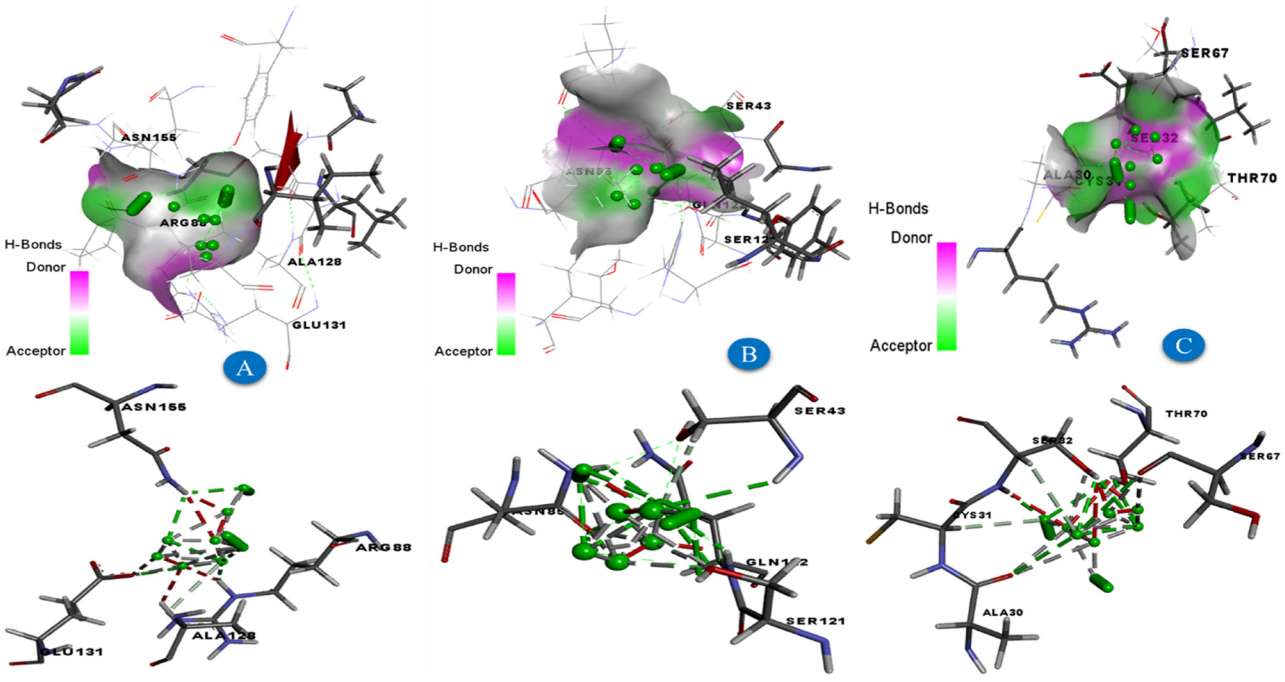

Figure 6: Molecular interaction of CuO-NPs and cutinase of *R. solani* (a), *F. oxysporum* (b), and *B. cinerea* (c).

areas: antibacterial properties, anticancer, cell imaging, and as a biocompatible delivery system [75].

3.6 Molecular docking interaction

Molecular docking interaction and scores are represented in Table 3 and Figure 5. CuO bound to the binding site of chitin synthase (Figure 5a), cutinase (Figure 6a), and agglutinin (Figure 7a) in *R. solani* by energy of −5.2, −4.3, and −4.7 kcal/mol, respectively. By −5.4, −5.1, and −5.0 kcal/mol, CuO interacted with the binding site of chitin synthase (Figure 5b), cutinase (Figure 6b), and trypsin (Figure 7b) in *F. oxysporum*, respectively. Regarding the *B. cinerea*'s chitin synthase (Figure 5c), cutinase (Figure 6c), and oxidoreductase (Figure 7c), CuO bound with their binding sites by −4.4, −4.8, and −5.1 kcal/mol, respectively.

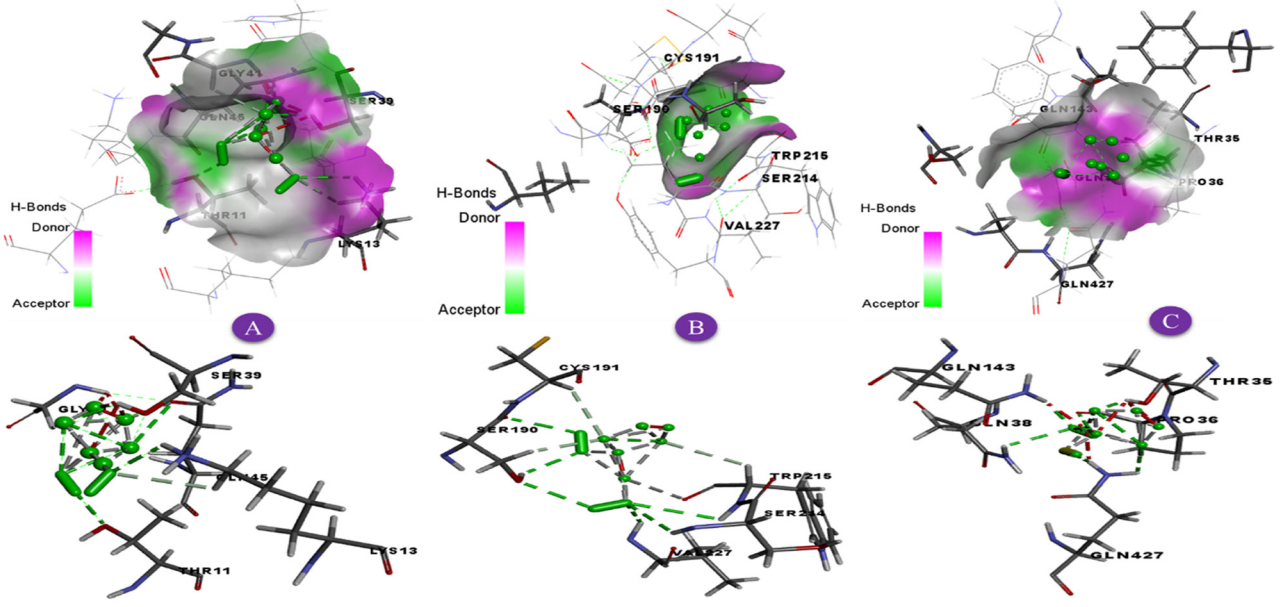

Figure 7: Molecular interaction of CuO-NPs and *R. solani* agglutinin (a), *F. oxysporum* trypsin (b), and *B. cinerea* oxidoreductase (c).

Targeting of fungal chitin synthase leads to loss of chitin in the fungal cell membrane and finally fungal death. Therefore, chitin synthesis is considered a promising target for antifungal drugs [76]. In addition, targeting oxidoreductases led to disturbances in fungal viability. Besides, fungal oxidoreductases play a major role in the pathogenicity and protection of fungi against host defense [77]. Fungal cutinase acts on cutin in the cuticle that covers all plant leaves, stems, flowers, and fruit [78]. Also, some antifungal agents possess trypsin inhibition and plant resistance against fungal attack [79]. Fungal agglutinin is a lectin accumulated in the mycelium and sclerotia fungi and serves as a storage protein [80]. In the current study, the molecular docking technique demonstrated that CuO has binding affinities for fungal trypsin. Furthermore, CuO exhibited binding affinities for fungal trypsin. Cutinase and agglutinin prevent the spreading of fungus on the infected strawberries.

4 Conclusions

Using an extract from *H. bacciferum* leaves, this study was able to make copper oxide nanoparticles (CuO-NPs). The CuO-NPs exhibited well-dispersed spherical particles with an average size of 24.8 ± 6.1 nm. The synthesized NPs displayed high concentrations of nanoscale copper ions, as confirmed by EDX analysis. Copper oxide nanoparticles produced with the help of *H. bacciferum* leaf extract have shown promising antifungal action against strawberry infections. The current work used molecular docking experiments to examine the interactions between the NPs and the target pathogens, revealing important details about their mechanism of action. The molecular docking model demonstrated CuO's affinity for engaging the binding sites of fungal target proteins, allowing researchers to investigate its antifungal potential. These interactions shed light on the putative mechanisms by which NPs exercise their antifungal effects. This information is critical for understanding the underlying mechanisms and enhancing the design of future antifungal NPs. Our findings show that copper oxide nanoparticles mediated by *H. bacciferum* leaf extract have the potential to be a practical and effective antifungal agent against strawberry infections. Further research and development in this area may result in the development of novel solutions for long-term crop protection and disease management in strawberry agriculture.

Acknowledgments: The authors express their sincere thanks to the City of Scientific Research and Technological Applications (SRTA-City) and the Faculty of Agriculture (Saba Basha), Alexandria University, Egypt, for providing the necessary research facilities. The authors would like to extend their appreciation to the Researchers Supporting Project number (RSP2024R505), King Saud University, Riyadh, Saudi Arabia.

Funding information: The research was financially supported by Researchers Supporting Project number (RSP2024R505), King Saud University, Riyadh, Saudi Arabia.

Author contributions: Study conception and design: A.A. and S.B.; data collection: E.H.l; analysis and interpretation of results: H.El., A.Al., P.K., and A.El.; and draft manuscript preparation: A.A., S.B., H.El., A.Al., and A.El. All authors reviewed the results and approved the final version of the manuscript.

Conflict of interest: The authors declare no conflict of interest.

Ethical approval: The conducted research is not related to either human or animals use.

Data availability statement: The datasets generated during and/or analysed during the current study are available from the corresponding author on reasonable request.

References

[1] El-Hefny M, Mohamed AA, Abdelkhalek A, Salem MZM. Productivity and phytochemicals of Asclepias curassavica in response to compost and silver nanoparticles application: HPLC analysis and antibacterial activity of extracts. Plants. 2023;12:2274.
[2] Tuutijärvi T, Lu J, Sillanpää M, Chen G. As (V) adsorption on maghemite nanoparticles. J Hazard Mater. 2009;166:1415–20.
[3] Nalwa HS. Nanostructured materials and nanotechnology: concise edition. San Diego, USA: Academic Press; 2001.
[4] Kanwar R, Rathee J, Salunke DB, Mehta SK. Green nanotechnology-driven drug delivery assemblies. ACS Omega. 2019;4:8804–15.
[5] Aseel DG, Behiry SI, Abdelkhalek A. Green and cost-effective nanomaterials synthesis from desert plants and their applications. Secondary Metabolites Based Green Synthesis of Nanomaterials and Their Applications. Singapore: Springer; 2023. p. 327–57.
[6] Husen A, Siddiqi KS. Advances in smart nanomaterials and their applications. Amsterdam: Elsevier; 2023. p. 337–50.
[7] Elkobrosy D, Al-Askar AA, El-Gendi H, Su Y, Nabil R, Abdelkhalek A, et al. Nematocidal and bactericidal activities of green synthesized silver nanoparticles mediated by Ficus sycomorus leaf extract. Life. 2023;13:1083.
[8] Ovais M, Khalil AT, Islam NU, Ahmad I, Ayaz M, Saravanan M, et al. Role of plant phytochemicals and microbial enzymes in biosynthesis of metallic nanoparticles. Appl Microbiol Biotechnol. 2018;102:6799–814.

[9] Huang J, Lin L, Sun D, Chen H, Yang D, Li Q. Bio-inspired synthesis of metal nanomaterials and applications. Chem Soc Rev. 2015;44:6330–74.
[10] Vaidehi D, Bhuvaneshwari V, Bharathi D, Sheetal BP. Antibacterial and photocatalytic activity of copper oxide nanoparticles synthesized using Solanum lycopersicum leaf extract. Mater Res Express. 2018;5:85403.
[11] Perreault F, Melegari SP, da Costa CH, Rossetto AL, de OF, Popovic R, et al. Genotoxic effects of copper oxide nanoparticles in Neuro 2A cell cultures. Sci Total Env. 2012;441:117–24.
[12] Nations S, Long M, Wages M, Maul JD, Theodorakis CW, Cobb GP. Subchronic and chronic developmental effects of copper oxide (CuO) nanoparticles on Xenopus laevis. Chemosphere. 2015;135:166–74.
[13] Al-Askar AA, Aseel DG, El-Gendi H, Sobhy S, Samy MA, Hamdy E, et al. Antiviral activity of biosynthesized silver nanoparticles from pomegranate (Punica granatum L.) peel extract against tobacco mosaic virus. Plants. 2023;12:2103.
[14] Tran TH, Nguyen VT. Copper oxide nanomaterials prepared by solution methods, some properties, and potential applications: A brief review. Int Sch Res Not. 2014;2014:1–14.
[15] Abdelkhalek A, El-Gendi H, Alotibi FO, Al-Askar AA, Elbeaino T, Behiry SI, et al. Ocimum basilicum-mediated synthesis of silver nanoparticles induces innate immune responses against cucumber mosaic virus in squash. Plants. 2022;11:2707.
[16] Lv Q, Zhang B, Xing X, Zhao Y, Cai R, Wang W, et al. Biosynthesis of copper nanoparticles using Shewanella loihica PV-4 with antibacterial activity: Novel approach and mechanisms investigation. J Hazard Mater. 2018;347:141–9.
[17] Mali SC, Dhaka A, Githala CK, Trivedi R. Green synthesis of copper nanoparticles using Celastrus paniculatus Willd. leaf extract and their photocatalytic and antifungal properties. Biotechnol Rep. 2020;27:e00518.
[18] Kamel SM, Elgobashy SF, Omara RI, Derbalah AS, Abdelfatah M, El-Shaer A, et al. Antifungal activity of copper oxide nanoparticles against root rot disease in cucumber. J Fungi. 2022;8:911.
[19] Siddiqui VU, Ansari A, Chauhan R, Siddiqi WA. Green synthesis of copper oxide (CuO) nanoparticles by Punica granatum peel extract. Mater Today Proc. 2021;36:751–5.
[20] Sathiyavimal S, Vasantharaj S, Bharathi D, Saravanan M, Manikandan E, Kumar SS, et al. Biogenesis of copper oxide nanoparticles (CuONPs) using Sida acuta and their incorporation over cotton fabrics to prevent the pathogenicity of Gram negative and Gram positive bacteria. J Photochem Photobiol B Biol. 2018;188:126–34.
[21] Ahmad S, AbdEl-Salam NM, Ullah R. *In vitro* antimicrobial bioassays, DPPH radical scavenging activity, and FTIR spectroscopy analysis of Heliotropium bacciferum. Biomed Res Int. 2016;2016:1–12.
[22] Iqbal K, Nawaz SA, Malik A, Riaz N, Mukhtar N, Mohammad P, et al. Isolation and lipoxygenase-inhibition studies of phenolic constituents from Ehretia obtusifolia. Chem Biodivers. 2005;2:104–11.
[23] Ahmad S, Ahmad S, Bibi A, Ishaq MS, Afridi MS, Kanwal F, et al. Phytochemical analysis, antioxidant activity, fatty acids composition, and functional group analysis of Heliotropium bacciferum. Sci World J. 2014;2014:1–8.
[24] Ahmad S, Bibi I, AbdEl-Salam NM, Hussain H, Ishaq MS, Adnan M, et al. Antibacterial and antifungal activities of the extract and fractions of aerial parts of Heliotropium bacciferum. Afr J Tradit Complement Altern Med. 2015;12:32–5.
[25] Chen J, Mao S, Xu Z, Ding W. Various antibacterial mechanisms of biosynthesized copper oxide nanoparticles against soilborne Ralstonia solanacearum. RSC Adv. 2019;9:3788–99. doi: 10.1039/c8ra09186b
[26] Möller EM, Bahnweg G, Sandermann H, Geiger HH. A simple and efficient protocol for isolation of high molecular weight DNA from filamentous fungi, fruit bodies, and infected plant tissues. Nucleic Acids Res. 1992;20:6115.
[27] Al-Askar AA, Bashir S, Mohamed AE, Sharaf OA, Nabil R, Su Y, et al. Antimicrobial efficacy and HPLC analysis of polyphenolic compounds in a whole-plant extract of Eryngium campestre. Separations. 2023;10:362.
[28] White TJ, Bruns T, Lee S, Taylor J. Amplification and direct sequencing of fungal ribosomal RNA genes for phylogenetics. PCR Protoc Guide Methods Appl. 1990;18:315–22.
[29] Grover RK, Moore JD. Toximetric studies of fungicides against BROWN rot organisms, sclerotinia-fructicola and S-Laxa. Phytopathology. 1962;52:876.
[30] Keabadile OP, Aremu AO, Elugoke SE, Fayemi OE. Green and traditional synthesis of copper oxide nanoparticles—comparative study. Nanomaterials. 2020;10:2502.
[31] Sardar M, Ahmed W, Al Ayoubi S, Nisa S, Bibi Y, Sabir M, et al. Fungicidal synergistic effect of biogenically synthesized zinc oxide and copper oxide nanoparticles against Alternaria citri causing citrus black rot disease. Saudi J Biol Sci. 2022;29:88–95. doi: 10.1016/j.sjbs.2021.08.067
[32] Gunalan S, Sivaraj R, Venckatesh R. Aloe barbadensis Miller mediated green synthesis of mono-disperse copper oxide nanoparticles: Optical properties. Spectrochim Acta Part A Mol Biomol Spectrosc. 2012;97:1140–4. doi: 10.1016/j.saa.2012.07.096
[33] Ali K, Ahmed B, Ansari SM, Saquib Q, Al-Khedhairy AA, Dwivedi S, et al. Comparative in situ ROS mediated killing of bacteria with bulk analogue, Eucalyptus leaf extract (ELE)-capped and bare surface copper oxide nanoparticles. Mater Sci Eng C. 2019;100:747–58.
[34] Ssekatawa K, Byarugaba DK, Angwe MK, Wampande EM, Ejobi F, Nxumalo E, et al. Phyto-mediated copper oxide nanoparticles for antibacterial, antioxidant and photocatalytic performances. Front Bioeng Biotechnol. 2022;10:820218.
[35] Meena PL, Chhachhia LK, Surela AK. Plant axillary stem gall extract mediated bioengineered CuO nanoprisms as robust and reusable catalyst for photocatalytic and catalytic degradation of water pollutants. J Mol Struct. 2024;1303:137575.
[36] Atri A, Echabaane M, Bouzidi A, Harabi I, Soucase BM, Chaâbane RB. Green synthesis of copper oxide nanoparticles using Ephedra Alata plant extract and a study of their antifungal, antibacterial activity and photocatalytic performance under sunlight. Heliyon. 2023;9:e13484.
[37] Roy SD, Das KC, Dhar SS. Facile synthesis of CuO-Ag2O hybrid metal oxide composite using carica papaya, cocooning with hydroxyapatite, and photocatalytic degradation of organic dyes. Mater Sci Eng B. 2024;303:117331.
[38] Talebian S, Shahnavaz B, Nejabat M, Abolhassani Y, Rassouli FB. Bacterial-mediated synthesis and characterization of copper oxide nanoparticles with antibacterial, antioxidant, and anticancer potentials. Front Bioeng Biotechnol. 2023;11:1140010.
[39] Manasa DJ, Chandrashekar KR, Madhu Kumar DJ, Niranjana M, Navada KM. Mussaenda frondosa L. mediated facile green synthesis of Copper oxide nanoparticles – Characterization, photocatalytic and their biological investigations. Arab J Chem. 2021;14:103184. doi: 10.1016/j.arabjc.2021.103184

[40] Yedurkar SM, Maurya CB, Mahanwar PA. A biological approach for the synthesis of copper oxide nanoparticles by Ixora coccinea leaf extract. J Mater Environ Sci. 2017;8:1173–8.
[41] Khatami M, Heli H, Mohammadzadeh Jahani P, Azizi H, Lima Nobre MA. Copper/copper oxide nanoparticles synthesis using Stachys lavandulifolia and its antibacterial activity. Iet Nanobiotechnol. 2017;11:709–13.
[42] Laha D, Pramanik A, Laskar A, Jana M, Pramanik P, Karmakar P. Shape-dependent bactericidal activity of copper oxide nanoparticle mediated by DNA and membrane damage. Mater Res Bull. 2014;59:185–91. doi: 10.1016/j.materresbull.2014.06.024
[43] Gaba S, Rai AK, Varma A, Prasad R, Goel A. Biocontrol potential of mycogenic copper oxide nanoparticles against Alternaria brassicae. Front Chem. 2022;10:966396.
[44] Weldegebrieal GK. Photocatalytic and antibacterial activity of CuO nanoparticles biosynthesized using Verbascum thapsus leaves extract. Optik (Stuttg). 2020;204:164230.
[45] Shankar SS, Ahmad A, Sastry M. Geranium leaf assisted biosynthesis of silver nanoparticles. Biotechnol Prog. 2003;19:1627–31.
[46] Ramesh P, Rajendran A. Photocatalytic dye degradation activities of green synthesis of cuprous oxide nanoparticles from Sargassum wightii extract. Chem Phys Impact. 2023;6:100208. doi: 10.1016/j.chphi.2023.100208
[47] Kumar PPNV, Shameem U, Kollu P, Kalyani RL, Pammi SVN. Green synthesis of copper oxide nanoparticles using Aloe vera leaf extract and its antibacterial activity against fish bacterial pathogens. Bionanoscience. 2015;5:135–9.
[48] Xu Y, Chen D, Jiao X, Xue K. CuO microflowers composed of nanosheets: Synthesis, characterization, and formation mechanism. Mater Res Bull. 2007;42:1723–31.
[49] Jaiswal M, Srivastava G, Mishra S, Kumar Singh P, Dhar R, Dabrowski R. Synthesis and characterization of semiconducting copper oxide nanoparticles and their impact on the physical properties of a nematic liquid crystalline material 4-pentyl-4′-cyanobiphenyl. J Mol Liq. 2023;383:122032. doi: 10.1016/j.molliq.2023.122032
[50] Veisi H, Karmakar B, Tamoradi T, Hemmati S, Hekmati M, Hamelian M. Biosynthesis of CuO nanoparticles using aqueous extract of herbal tea (Stachys Lavandulifolia) flowers and evaluation of its catalytic activity. Sci Rep. 2021;11:1983.
[51] Král'ová K, Jampílek J. Medicinal and aromatic plant species with potential for remediation of metal (loid)-contaminated soils. Sustainable Management of Environmental Contaminants. Eco-friendly Remediation Approaches. Cham, Switzerland: Springer; 2022. p. 173–236.
[52] Mohamed EA. Green synthesis of copper & copper oxide nanoparticles using the extract of seedless dates. Heliyon. 2020;6:e03123.
[53] Halawani EM. Rapid biosynthesis method and characterization of silver nanoparticles using Zizyphus spina christi leaf extract and their antibacterial efficacy in therapeutic application. J Biomater Nanobiotechnol. 2016;8:22–35.
[54] Swarna SS, Govindarajan VU, Anbalagan A, Christopher D, Muthuraman MS. Green synthesis of copper oxide nanoparticles using Ziziphus oenoplia extract and its dye degradation properties. Biomass Convers Biorefin. 2024;14:1–12.
[55] Padil VVT, Černík M. Green synthesis of copper oxide nanoparticles using gum karaya as a biotemplate and their antibacterial application. Int J Nanomed. 2013;8:889–98.
[56] Weldegebrieal GK. Photocatalytic and antibacterial activityof CuO nanoparticles biosynthesized using Verbascum thapsus leaves extract. Optik (Stuttg). 2020;204:164230.
[57] Topnani N, Kushwaha S, Athar T. Wet synthesis of copper oxide nanopowder. Int J Green Nanotechnol Mater Sci Eng. 2010;1:M67–73.
[58] Moni ZR, Ali MA, Alam MS, Rahman MA, Bhuiyan MR, Mian MS, et al. Morphological and genetical variability among Rhizoctonia solani isolates causing sheath blight disease of rice. Rice Sci. 2016;23:42–50.
[59] Desvani SD, Lestari IB, Wibowo HR, Supyani S, Poromarto SH, Hadiwiyono H. Morphological characteristics and virulence of Rhizoctonia solani isolates collected from some rice production areas in some districts of Central Java. AIP Conf. Proc. 2014, AIP Publishing LLC; 2018. p. 20068.
[60] Ke X, Lu M, Wang J. Identification of Fusarium solani species complex from infected zebrafish (Danio rerio). J Vet Diagn Investig. 2016;28:688–92.
[61] Leslie JF, Summerell BA. The fusarium laboratory manual. Ames, Iowa, USA: John Wiley & Sons; 2007. doi: 10.1002/9780470278376.
[62] Elad Y, Williamson B, Tudzynski P, Delen N. Botrytis spp. and diseases they cause in agricultural systems–an introduction. In Botrytis: Biology, Pathology and Control. Dordrecht, The Netherlands: Springer; 2007. p 1–8.
[63] Notte A-M, Plaza V, Marambio-Alvarado B, Olivares-Urbina L, Poblete-Morales M, Silva-Moreno E, et al. Molecular identification and characterization of Botrytis cinerea associated to the endemic flora of semi-desert climate in Chile. Curr Res Microb Sci. 2021;2:100049.
[64] Al-Abedy AN, Al-Fadhal FA, Karem MH, Al–Masoudi Z, Al-Mamoori SA. Genetic variability of different isolates of Rhizoctonia solani Kühn isolated from Iranian imported potato tubers (Solanum tuberosum L.). Int J Agric Stat Sci. 2018;14:587–98.
[65] Khan M, Wang R, Li B, Liu P, Weng Q, Chen Q. Comparative evaluation of the LAMP assay and PCR-based assays for the rapid detection of Alternaria solani. Front Microbiol. 2018;9:2089.
[66] Schocha CL, Seifertb KA, Huhndorfc S, Robertd V, Spougea JL, Levesqueb CA, et al. Nuclear ribosomal internal transcribed spacer (ITS) region as a universal DNA barcode marker for Fungi. PNAS. 2012;109:6241–6.
[67] Tedersoo L, Bahram M, Dickie IA. Does host plant richness explain diversity of ectomycorrhizal fungi? Re-evaluation of Gao et al. (2013) data sets reveals sampling effects. Mol Ecol. 2014;23:992–5.
[68] Jebril S, Jenana RKB, Dridi C. Green synthesis of silver nanoparticles using Melia azedarach leaf extract and their antifungal activities: *In vitro* and *in vivo*. Mater Chem Phys. 2020;248:122898.
[69] Zhu W, Hu C, Ren Y, Lu Y, Song Y, Ji Y, et al. Green synthesis of zinc oxide nanoparticles using Cinnamomum camphora (L.) Presl leaf extracts and its antifungal activity. J Env Chem Eng. 2021;9:106659.
[70] Anand GT, Renuka D, Ramesh R, Anandaraj L, Sundaram SJ, Ramalingam G, et al. Green synthesis of ZnO nanoparticle using Prunus dulcis (Almond Gum) for antimicrobial and supercapacitor applications. Surf Interfaces. 2019;17:100376.
[71] Ashraf A, Fatima N, Shahzadi I, Tariq H, Shahzadi A, Yameen MA, et al. Datura suaveolens and Verbena tenuisecta mediated silver nanoparticles, their photodynamic cytotoxic and antimicrobial evaluation. World J Microbiol Biotechnol. 2020;36:1–12.
[72] Ballottin D, Fulaz S, Cabrini F, Tsukamoto J, Duran N, Alves OL, et al. Antimicrobial textiles: Biogenic silver nanoparticles against Candida and Xanthomonas. Mater Sci Eng C. 2017;75:582–9.

[73] Ravichandran V, Vasanthi S, Shalini S, Shah SAA, Tripathy M, Paliwal N. Green synthesis, characterization, antibacterial, antioxidant and photocatalytic activity of Parkia speciosa leaves extract mediated silver nanoparticles. Results Phys. 2019;15:102565.
[74] Punniyakotti P, Panneerselvam P, Perumal D, Aruliah R, Angaiah S. Anti-bacterial and anti-biofilm properties of green synthesized copper nanoparticles from Cardiospermum halicacabum leaf extract. Bioprocess Biosyst Eng. 2020;43:1649–57.
[75] Mukherjee S, Chowdhury D, Kotcherlakota R, Patra S, Vinothkumar B, Bhadra MP, et al. Potential theranostics application of bio-synthesized silver nanoparticles (4-in-1 system). Theranostics. 2014;4:316–35. doi: 10.7150/thno.7819.
[76] Ruiz-Herrera J, San-Blas G. Chitin synthesis as target for antifungal drugs. Curr Drug Targets Infect Disord. 2003;3:77–91. doi: 10.2174/1568005033342064.
[77] Yu Q-K, Han L-T, Wu Y-J, Liu T-B. The role of oxidoreductase-like protein olp1 in sexual reproduction and virulence of Cryptococcus neoformans. Microorganisms. 2020;8:1730. doi: 10.3390/microorganisms8111730.
[78] Niklas KJ, Cobb ED, Matas AJ. The evolution of hydrophobic cell wall biopolymers: From algae to angiosperms. J Exp Bot. 2017;68:5261–9. doi: 10.1093/jxb/erx215.
[79] Marcela Giudici A, Clelia Regente M, de la Canal L. A potent antifungal protein from Helianthus annuus flowersis a trypsin inhibitor. Plant Physiol Biochem. 2000;38:881–8. doi: 10.1016/S0981-9428(00)01191-8.
[80] Skamnaki VT, Peumans WJ, Kantsadi AL, Cubeta MA, Plas K, Pakala S, et al. Structural analysis of the Rhizoctonia solani agglutinin reveals a domain-swapping dimeric assembly. FEBS J. 2013;280:1750–63. doi: 10.1111/febs.12190.